

A Chandra Observation of the Nearby Lenticular Galaxy NGC 5102: Where are the X-ray Binaries?

R. P. Kraft

Harvard/Smithsonian Center for Astrophysics, 60 Garden St., MS-67, Cambridge, MA 02138

L. A. Nolan, T. J. Ponman

School of Physics and Astronomy, University of Birmingham, Birmingham, B15 2TT, UK

C. Jones

Harvard/Smithsonian Center for Astrophysics, 60 Garden St., Cambridge, MA 02138

S. Raychaudhury

School of Physics and Astronomy, University of Birmingham, Birmingham, B15 2TT, UK

ABSTRACT

We present results from a 34 ks Chandra/ACIS-S observation of the LMXB population and the hot ISM in the nearby ($d=3.1$ Mpc) lenticular galaxy NGC 5102, previously shown to have an unusually low X-ray luminosity. We detect eleven X-ray point sources within the the D_{25} optical boundary of the galaxy (93% of the light), one third to one half of which are likely to be background AGN. One of the X-ray sources is coincident with the optical nucleus and may be a low-luminosity AGN. Only two sources with an X-ray luminosity greater than 10^{37} ergs s^{-1} in the 0.5-5.0 keV band were detected, one of which is statistically likely to be a background AGN. We expected to detect 7 or 5 such luminous sources if the XRB population scales linearly with the B band or J band magnitudes, respectively, of the host galaxy. By this measure, NGC 5102 has an unusually low number of XRBs. The deficit of LMXBs is even more striking because some of these sources may in fact be HMXBs. NGC 5102 is unusually blue for its morphological type, and has undergone at least two recent bursts of star formation only $\sim 1.5 \times 10^7$ and $\sim 3 \times 10^8$ years ago. We present the results of optical/UV spectral synthesis analysis and demonstrate that a significant fraction ($>50\%$) of the stars in this galaxy are comparatively young ($<3 \times 10^9$ years old). We discuss the relationship between the XRB population, the globular

cluster population, and the relative youth of the majority of stars in this galaxy. If the lack of X-ray binaries is related to the relative youth of most of the stars, this would support models of LMXB formation and evolution that require wide binaries to shed angular momentum on a timescale of Gyrs. We have also analyzed archival HST images of NGC 5102, and find that it has an unusually low specific frequency of globular clusters ($S_N \sim 0.4$). The lack of LMXBs could also be explained by the small number of GCs. We have also detected diffuse X-ray emission in the central ~ 1 kpc of the galaxy with an X-ray luminosity of 4.1×10^{37} ergs s^{-1} in the 0.1-2.0 keV band. This hot gas is most likely a superbubble created by multiple supernovae of massive stars born during the most recent star burst, and is driving the shock into the ISM which was inferred from previous [O III] $\lambda 5007$ and H_α observations.

Subject headings: galaxies: individual (NGC 5102) - X-rays: galaxies - galaxies: ISM

1. Introduction

Early-type galaxies have been known to be luminous X-ray sources since the Einstein era. The X-ray emission from the most massive elliptical galaxies is dominated by emission from thermal coronae. These coronae may be primordial and enriched with metals from outflows created by supernovae or stellar winds, or they may be entirely built up from such outflows, with the primordial gas being blown off during a large, early burst of star formation (David, Forman, & Jones 1990, 1991; O’Sullivan, Forbes, & Ponman 2001). There is a well known correlation between the X-ray luminosity of an elliptical galaxy and its total mass (quantified by its blue magnitude), although there is more than a factor of 100 dispersion around the mean. For less massive galaxies, and for massive galaxies that have lost much of their corona through tidal or ram pressure stripping, the contribution of the population of X-ray binaries (XRB) to the total X-ray luminosity becomes increasingly important. The contribution of the XRB population to the X-ray spectra of early galaxies was noted in Einstein and ASCA observations (Kim, Fabbiano, & Trinchieri 1992; Matsumoto *et al.* 1997). The Chandra X-ray Observatory (CXO) has observed a large number of elliptical and S0 galaxies and has resolved the brightest XRBs from the hot ISM (e.g. Sarazin, Irwin, & Bregman (2000); Kraft *et al.* (2001); Kundu, Maccarone, & Zepf (2002) among many others). The XRB populations of galaxies with a range of masses and morphological types have now been studied in detail, and it is clear that the variance in the number of XRBs per unit optical luminosity in early galaxies is larger than that expected based on counting statistics alone.

This variance is likely related to the origin and evolution of the XRBs, subjects on which there is still considerable debate.

There is general agreement that the creation of XRBs must be a continuous, ongoing phenomenon in the life cycle of early galaxies because the lifetime of all XRBs is considerably less ($\sim 10^9$ yrs for low mass X-ray binaries (LMXBs) and $\sim 10^7$ yrs for high mass X-ray binaries) than the age of their host galaxy (Grimm, Gilfanov, & Sunyaev 2002). The specific mechanism for XRB formation is still a subject of contention. Some have argued that most or all of the XRBs in elliptical galaxies originate in globular clusters because they are the only regions where the stellar density is sufficient for neutron stars to be captured in N-body interactions. Recent Chandra observations of NGC 4472, NGC 1399, and other massive early galaxies have shown that a significant (40-60%) fraction of the XRBs are coincident with globular clusters, supporting this idea. In this scenario, the variance in the number of XRBs can then be explained as differences in the globular cluster populations. However, the ellipticals for which a large XRB/GC correlation have been demonstrated are located in rich environments and have exceptionally large globular cluster specific frequencies (GCSFs). Even in early-type galaxies with unusually large GCSFs, at least half of the XRB population is not directly accounted for by this GC/XRB correlation. Others have argued that the XRB population is related to the bulk of the stars in the galaxy, and that the variance in the XRB populations is related to the star formation history of the host galaxy (White & Ghosh 1998; Wu 2001). The fact that the majority of the LMXBs in the galactic center region of the Milky Way and the M31 bulge do not appear to be associated with GCs supports this argument. Recent analysis of the X-ray point source population from a sample of early galaxies suggests both mechanisms are important (Irwin & Bregman 2004).

In this paper, we present results from a 34 ks Chandra/ACIS-S observation of the S0 galaxy NGC 5102. NGC 5102 is a small ($M_B = -17.45$) nearby ($d = 3.1 \pm 0.15$ (McMillan, Ciardullo, & Jacoby 1995)) lenticular galaxy and is a member of the Centaurus A group (Israel 1998). The luminosity of this galaxy, and therefore presumably the mass, is similar to the LMC. NGC 5102 has been previously observed by Einstein and ROSAT (Forman, Jones, & Tucker 1985; Irwin & Sarazin 1998; O’Sullivan, Forbes, & Ponman 2001), where it was noted that its integrated X-ray luminosity is considerably less than one would expect from a simple extrapolation of its mass compared with the more luminous ellipticals. The bulge of this galaxy is unusually blue for its morphological type, and it is believed to have undergone one or more recent bursts of star formation (within $\sim 10^8$ years ago), although spectral synthesis modeling suggests that most or all of the stars are relatively young ($< 5 \times 10^9$ yrs) (Pritchett 1979; Rocca-Volmerange & Guiderdoni 1987; Deharveng *et al.* 1997). Note that unlike most other early-type galaxies, it is possible that NGC 5102 has a significant HMXB population because of the recent star formation. In order to better understand the

link between the XRB populations, the GC population, and the star formation history of the stellar population, we have analyzed archival HST data to search for GCs and made a spectral stellar synthesis study of the optical/UV spectra of the galaxy to constrain the star formation history.

The purpose of this observation was two-fold. The primary goal was to resolve the XRB population from the hot gas and quantify the nature of the X-ray deficit in this unusually blue galaxy. Because of the proximity of the galaxy and the sensitivity of the CXO, we have been able to detect point sources below $L_X \sim 10^{36}$ ergs s^{-1} , much deeper than most Chandra observations of more massive early-type galaxies at the distance of the Virgo cluster. We wanted to compare the XRB population of this galaxy with other early-type galaxies observed with Chandra. Naively, one would expect that the recent bursts of star formation might enhance the XRB population relative to older ellipticals due to the presence of the additional population of HMXBs. On the contrary, there are surprisingly few XRBs. A secondary goal of this observation was to resolve any hot gas that may be present in the galaxy from the XRB population, and to determine its thermodynamic state.

This paper is organized as follows. Section 2 contains a brief discussion of the observation and data preparation. The X-ray point source (XPS) population and its luminosity function are presented in section 3. Spectral and spatial analysis of the hot ISM is described in section 4. A discussion of the significance of the lack of XRBs, particularly as it relates both to the stellar ages and star formation history as derived from optical/UV spectral synthesis and to the GC population, is presented in section 5. We conclude with a brief discussion and implications of our results in section 6. We assume a distance to NGC 5102 of 3.1 Mpc throughout this paper (McMillan, Ciardullo, & Jacoby 1995), and J2000 coordinates are used in all figures and tables.

2. Observation Log

The lenticular galaxy NGC 5102 was observed by the Chandra X-ray Observatory for 34217 s with the ACIS-S detector in very faint (VF) mode. A summary of the optical properties of NGC 5102 and the Chandra observing log are contained in Table 1. Very faint mode event filtering was applied to the data to reduce the background to the lowest possible levels. Hot columns, events near node boundaries, short term transients, and the streaks on the S4 chip were also removed. The background above 2 keV was examined for periods of flaring and none were found. The level of the background in the 2-10 keV band agrees well with the nominal blank-sky ACIS-S background. A 2MASS J-band image with the FOV of the ACIS S2, S3, and S4 CCDs overlaid is shown in Figure 1.

3. X-ray Point Sources

Individual point sources were detected with the CIAO program *wavdetect* in the 0.5-5.0 keV band. The detection sensitivity was chosen so that there is approximately one false detection for every million pixels. The source list generated by *wavdetect* was visually compared with a raw image to confirm that every source it detected was indeed a source. We likewise inspected the raw image to ensure that all sources visible by eye were detected by the program. We detected 55 sources within the intersection of a $12.2' \times 13.0'$ box centered on the galaxy and the ACIS-S FOV (see Figure 1). Based on the sensitivity, we expect one of these to be a false source. To convert the observed count rate to flux, we have assumed a 5 keV thermal bremsstrahlung spectrum with galactic ($N_H = 5 \times 10^{20} \text{ cm}^{-2}$) absorption, a spectrum typical of LMXBs. For this spectrum, a count rate of $10^{-3} \text{ cts s}^{-1}$ in the 0.5-5 keV band corresponds to a flux (unabsorbed) of $7.04 \times 10^{-15} \text{ ergs cm}^{-2} \text{ s}^{-1}$ in the same band. We define the boundary of the galaxy to be the D_{25} isophote (de Vaucouleurs *et al.* 1991). The major and minor effective diameters at this isophote are $8.7'$ and $2.8'$, respectively, and the apparent diameter of the effective aperture is $0.79'$. Assuming that the light is distributed according to the de Vaucouleurs $R^{1/4}$ law, this ellipse contains approximately 93% of the light. The positions, count rates and uncertainties, and X-ray luminosities (if the source is located within the D_{25} boundary) of the sources are shown in Table 2. The D_{25} isophote is contained entirely within the S3 chip. Several of the sources outside this boundary appear to be coincident with foreground stars in 2MASS and DSS images. We note that several of the sources (labeled with a dagger in Table 2) were detected on the S2 and S4 chips. For these sources (assuming the same spectrum and correcting for vignetting), a count rate of $10^{-3} \text{ cts s}^{-1}$ in the 0.5-5 keV band corresponds to a flux (unabsorbed) of $1.06 \times 10^{-14} \text{ ergs cm}^{-2} \text{ s}^{-1}$ in the same band.

Only eleven X-ray point sources (XPSs) are contained within the D_{25} boundary of the galaxy (all on the S3 chip), and only two sources with $L_X \geq 10^{37} \text{ ergs s}^{-1}$ in the 0.5-5.0 keV band. A 2MASS J band image with the positions of all of the sources overplotted is shown in Figure 2. The positions of HII regions and planetary nebulae (PN) have also been overplotted for visual comparison (McMillan, Ciardullo, & Jacoby 1995). There are no co-incidences between the XPSs and any of the HII regions or PN. Two of the XPSs are located near the optical center of the galaxy. One of the sources is one of the two sources with $L_X > 10^{37} \text{ ergs s}^{-1}$, and the other, less luminous source is coincident with the optical center/nucleus. It is possible that this second source is a low-luminosity AGN (LLAGN), although no other evidence of nuclear activity has been reported in the literature. There is a group of sources approximately $3.5'$ north of the center of the galaxy, but whether this group is related to NGC 5102 is not known.

The luminosity function (LF) of the XPSs contained within the optical boundary of the galaxy is plotted in Figure 3. A significant fraction of these are likely to be background AGN unrelated to NGC 5102. We have overplotted an estimate of the number of background AGN onto Figure 3 based on number counts from deep observations of the Chandra Deep Field South (Tozzi *et al.* 2001). Note that the source fluxes have been scaled in this figure to the 0.5-2.0 keV band in order to simplify comparison with the deep survey results. Our point source detection is complete and unbiased, defined as a 4σ measurement of the luminosity (see Kraft *et al.* (2001) for details) above a luminosity of $L_X=4\times 10^{36}$ ergs s^{-1} . Above this luminosity, two of our three sources are statistically likely to be background AGN. Half of the sources in the LF shown in Figure 3 were detected with less than 10 counts. A detailed statistical comparison between the LF of the galactic sources and the background AGN would require an extensive Monte Carlo simulation to assess the effects of various biases introduced by low number counting statistics (see Kenter & Murray (2003) for a detailed discussion of these biases and references). The details of this are not significant for our discussion below, and such an analysis is beyond the scope of this paper. We conclude that of the 11 detected sources, it is likely that a significant fraction are background objects unrelated to NGC 5102. Based on an examination of the HST images (described below), source #17 is likely to be an unrelated background galaxy. Beyond the optical boundary of the galaxy, the surface density of X-ray sources is approximately consistent with the deep survey results. The integrated X-ray luminosity of the eleven sources contained within the optical boundary of the galaxy is 5.6×10^{37} ergs s^{-1} in the 0.5-5 keV band.

NGC 5102 has considerably fewer XRBs than expected based on a linear extrapolation from more massive early-type galaxies. To quantitatively demonstrate this we compare the number of XRBs with $L_X \geq 10^{37}$ ergs s^{-1} to that observed in Cen A (Kraft *et al.* 2001, 2005) and estimated from an extrapolation of the XRB luminosity function in NGC 4472 (Maccarone, Kundu, & Zepf 2003). As shown in Figure 3, we have detected two sources within the boundary of the galaxy with $L_X \geq 10^{37}$ ergs s^{-1} , one of which is statistically likely to be an unrelated background AGN. It is possible that both or neither of these sources are related to NGC 5102, but for the purposes of this analysis, we will assume that one of the sources is related to the galaxy, and one is an unrelated background object. The choice of $L_X \geq 10^{37}$ ergs s^{-1} as the limiting luminosity for our comparison is well above our completeness threshold so that the biases described in the previous paragraph are insignificant. An XRB with a luminosity of 10^{37} ergs s^{-1} at the distance of NGC 5102 corresponds to a source with 43 counts in our ~ 34 ks observation. We have not missed any sources with $L_X > 10^{37}$ ergs s^{-1} associated with the galaxy, and the uncertainty in the estimation of luminosity is an insignificant source of systematic error.

The apparent and absolute luminosities in the J and B bands of NGC 5102, Cen A,

and NGC 4472 are summarized in Table 3. Approximately 110 XRBs were detected in Cen A with $L_X > 10^{37}$ ergs s^{-1} (this is probably a slight underestimate because the distant halo was beyond the FOV of these observations), and we estimate that there are ~ 220 such XRBs in NGC 4472 based on an extrapolation of the luminosity function (Figure 4 of Kundu, Maccarone, & Zepf (2002)) to this luminosity. Scaling these values by the ratio of B band luminosity, we expect to detect 6 such LMXBs in NGC 5102. We have detected one. As stated above, NGC 5102 is unusually blue because of bursts of recent star formation. A similar scaling by J band luminosity predicts 5 such LMXBs in NGC 5102. The Poisson probability of observing 1 XRB if the mean is 5 is not unreasonably low ($\sim 3.4\%$), but improbable. We are certainly in the regime of small number statistics, but emphasize that this result is in general agreement with that of Irwin & Sarazin (1998) who found that the X-ray luminosity (above 0.5 keV) of NGC 5102 is less than predicted based on extrapolation from higher mass objects. Possible explanations for this result are discussed below. The lack of XRBs cannot be a general result related to lower mass elliptical and/or lenticular galaxies because there are several similar galaxies that have a hard X-ray component in their spectra that are consistent with an extrapolation to higher mass galaxies (O’Sullivan, Forbes, & Ponman 2001).

The XLF below 10^{37} ergs s^{-1} gives us additional information, but it is more difficult to make a quantitative comparison because there are few observations of other galaxies to this limiting luminosity. We have detected approximately 6-9 objects in NGC 5102 with $36 < \log(L_X(\text{ergs } s^{-1})) < 37$ (see the discussion above). If we extrapolate the XLF of Cen A down to a limiting luminosity of 10^{36} ergs s^{-1} and scale by blue luminosity, we would expect about fifty sources with $36 < \log(L_X(\text{ergs } s^{-1})) < 37$ in NGC 5102. We note that this is only an extrapolation, and that the power law index in this luminosity range is not known, although there is a suggestion that it flattens out (see Figure 8 of Kraft *et al.* (2001)). CXO observations of the bulge of M31 detect a clear flattening of the power law index (Kong *et al.* 2003) in this luminosity range. The paucity of sources in NGC 5102 in the luminosity range $36 < \log(L_X(\text{ergs } s^{-1})) < 37$ may or may not be typical of early galaxies in general, but there is certainly not a large (~ 25 -50) population of sources in this luminosity range, with a drastic steepening of the LF power law index above 10^{37} ergs s^{-1} .

4. Diffuse Emission

We have created an adaptively smoothed, exposure corrected X-ray image in the 0.5-2.0 keV band with the point sources removed. Contours from this images are overlaid onto a 2MASS J band image in Figure 4. The diffuse emission is centrally peaked and centered

on the optical/IR center of the galaxy. There are too few counts in the diffuse emission to constrain model parameters of a surface brightness profile fit (e.g. a β -model) in a meaningful way. We extracted a spectrum of the unresolved emission from a region $1'$ (900 pc) in radius centered on the optical center of the galaxy. Background was determined from an identical sized region on the S3 chip away from the galaxy. Hypothesising that the emission is due to hot gas, we fit the spectrum with an absorbed APEC model using XSPEC (V11) holding the absorption constant at the galactic value ($5 \times 10^{20} \text{ cm}^{-2}$). The elemental abundance was also held fixed at 0.4 relative to solar. Additional fits were performed with one or both of these parameters free, but they were not constrained in a meaningful way, although they generally preferred a low (< 0.05) value for the abundance. The low abundance is commonly interpreted as indicating the presence of multi-temperature gas with spatially varying abundances (Fabbiano *et al.* 2003).

The best fit temperature is $0.31_{-0.07}^{+0.23}$ keV (90% confidence for abundance fixed at 0.4 times solar), and the density of the gas is $n_H = 7.2 \times 10^{-3} \text{ cm}^{-3}$ assuming the gas is uniform throughout this region and that $n_H = 1.18 n_e$, appropriate for an ionized plasma with subsolar abundances. From Figure 4, it is clear that the surface brightness of the gas is centrally peaked. The X-ray luminosity of the gas is $4.1 \times 10^{37} \text{ ergs s}^{-1}$ (unabsorbed) in the 0.1 to 2.0 keV band. We note that this is more than an order of magnitude less than the luminosity estimate of Irwin & Sarazin (1998). Much of this difference can be accounted for by differences in the assumed distance to NGC 5102 and the measured gas temperature. It is possible that there is additional cooler gas present in NGC 5102 to which the ACIS-S instrument is not particularly sensitive. The sensitivity of the ACIS-S has been gradually reduced because of the build-up of contamination. In any case, the ROSAT PSPC had considerably more effective area than Chandra/ACIS-S below 0.5 keV. The addition of a second, lower temperature ($T < 0.1 \text{ keV}$) component marginally improves the quality of the fits, but the limited statistics prevent us from making a quantitative statement. The low temperature argues against this diffuse emission actually being a population of unresolved, lower luminosity X-ray binaries.

This hot ISM may be related to the ring-like feature seen in optical emission lines by van den Bergh (1976) and McMillan, Ciardullo, & Jacoby (1995). They detected an asymmetric ring-like structure in [O III] $\lambda 5007$ and H_α emission extending approximately 0.7 kpc from the nucleus. The preferred model of McMillan, Ciardullo, & Jacoby (1995) for the origin of this emission was shock excitation from an expanding super bubble. The expansion velocity was estimated at 60 km s^{-1} from optical line ratios. We suggest that the X-ray gas is this superbubble which was created as a result of the most recent epoch of star formation. The expansion of this hot gas is responsible for shock heating the ISM and the appearance of the emission line structures. The total mass and thermal energy of the hot gas is $\sim 10^6 M_\odot$

and $\sim 10^{54}$ ergs, respectively. These values are close to the estimates of the total mass and energy of the starburst in the nuclear region (McMillan, Ciardullo, & Jacoby 1995). The fact that the X-ray emission is centered on the nucleus supports the hypothesis that it is related to a nuclear starburst, and not to some type of phenomenon in the bulge. This bulge phenomenon was invoked by McMillan, Ciardullo, & Jacoby (1995) to explain how the ring-like structure could have survived 2×10^8 yrs against differential rotation. At a velocity of only 60 km s^{-1} , the structures could only be about 10^7 yrs old. More recent optical and UV observations suggest that the time since the last starburst was only 15 Myrs (Deharveng *et al.* 1997).

5. LMXB Formation: Star Formation History versus Globular Clusters

The apparent lack of XRBs in NGC 5102 gives information about the details of their formation and evolution. The standard paradigm is that the majority of the luminous XRBs in elliptical and lenticular galaxies are low mass X-ray binaries: neutron stars accreting matter via Roche lobe overflow from a nearby late type stellar companion, such as Sco X-1 or Cyg X-2 in our galaxy. The details of the origin and evolution of these X-ray binaries are still poorly understood and the subject of considerable debate. The lifetime of a neutron star accreting matter from a late-type dwarf with $L_X > 10^{37} \text{ ergs s}^{-1}$ is only $\sim 10^9$ yrs, so that either the XRB phenomenon is intrinsically transient (i.e. we are presently observing only a small number of the XRBs present), XRBs are being continuously created during the lifetime of a galaxy, or the emission of many of the XRBs is beamed so that we have greatly overestimated their luminosities and therefore underestimated their lifetimes. This third phenomenon does not appear to be important for the vast majority of luminous LMXBs in our galaxy and it will not be considered further here. The temporal variability and evolution of a large population of XRBs outside the Milky Way is only now beginning to be studied with Chandra. It is possible that we have been unlucky and observed NGC 5102 during a period when an unusually large number of LMXBs are in quiescence. However, unless the temporal properties of the LMXBs in NGC 5102 are for some reason different from those in other early galaxies, this is improbable. Long term monitoring the XRB population of the Milky Way and Cen A suggests that any snapshot of the entire XRB population is a representative sample even though many of the individual sources may be highly variable (Grimm, Zezas, & Fabbiano 2004; Kraft *et al.* 2005). Thus, differences in the XRB populations among galaxies is likely related to their formation and evolution.

The formation and evolution of LMXBs is thought to proceed along one of two general lines. On the one hand, it has been proposed that the majority of XRBs in early galaxies

are formed in globular clusters, the only region where the stellar densities are sufficient to create such systems via N-body interactions (White, Sarazin, & Kulkarni 2002; Maccarone, Kundu, & Zepf 2003). Recent observations of nearby, massive elliptical galaxies support this claim and find that 30-60% of the luminous XRBs are coincident with globular clusters, although only 3-4% of the GCs contain X-ray sources (Angelini, Loewenstein, & Mushotzky 2001; Maccarone, Kundu, & Zepf 2003). White, Sarazin, & Kulkarni (2002) found a positive correlation between L_{LMXB}/L_{OPT} ratios and globular cluster specific frequency. As an alternative, it has been argued that the LMXB population of early galaxies is related to the star formation history of the host galaxy (White & Ghosh 1998; Wu 2001). A variety of scenarios have been developed to explain the evolution of close binary systems and the subsequent creation of LMXBs (Webbink, Rappaport, Savonijie 1983; Kalogera & Webbink 1996, 1998). Generally, the LMXB begins as a wide binary with a large mass ratio. The more massive star rapidly proceeds through its lifecycle and explodes as a supernova. The orbit of the binary decays, perhaps through magnetic braking, until Roche lobe overflow occurs and the LMXB is born. The luminosity function contains information on the birth/death rate of XRBs and on past epochs of star formation. The XRBs should be distributed roughly as the optical starlight in this scenario. This hypothesis is supported by the fact that the majority of the LMXBs in the bulges of both the Milky Way and M31 do not appear to be related to GCs. Both components are likely to play an important role, the relative importance of each for any individual galaxy may depend on a wide range of factors such as environment, star formation history, etc.

In order to assess the applicability of these two general models to the unusual case of NGC 5102, we have analyzed archival HST imaging data to study the GC population, and have used stellar spectral synthesis analysis on the UV/optical spectrum of the galaxy to constrain its star formation history. We find that the majority of the stellar population is young, and that NGC 5102 has an unusually small number of GCs. Either of these could explain the deficit of X-ray sources.

5.1. Stellar Spectral Synthesis

Given the unusual color of this galaxy, it is interesting to determine its star formation history and ask whether the deficit of XRBs is related to this history. In order to evaluate any potential relationship between the deficit of XRBs in NGC 5102 and its star formation history, we have estimated the age of the stellar populations of the galaxy by fitting a two component stellar population evolutionary synthesis model to the UV-optical spectrum of this galaxy. In a future publication, we will present the results of a more comprehensive

comparison of the XRB population and the star formation history derived from spectral synthesis of a large sample of early galaxies. The UV and optical data of NGC 5102 were taken from several archival sources as described in Table 4. Adjacent spectral sections were normalized to unity in the region of wavelength overlap spliced together. The data are corrected for Galactic reddening. The errors in the flux are the observed errors for the IUE data ($\lambda \leq 3100 \text{ \AA}$), and are estimated at 6% of the observed flux for the optical data ($\lambda > 3100 \text{ \AA}$). There is sufficient data in the long-baseline spectrum to allow the robust disentanglement of multiple stellar populations. A two-component stellar population evolutionary synthesis model was constructed, using the instantaneous starburst models of Jimenez et al. (1998). These have ages ranging from 0.01 – 14 Gyr, and metallicities 0.01, 0.2, 0.5, 1.0, 1.5, 2.5 and $5.0 Z_{\odot}$. Age, metallicity and fractional contribution by (stellar) mass of each component of the composite model were allowed to vary as free parameters. The details of this technique are presented elsewhere (Dunlop *et al.*, 2005, in preparation).

Figure 5 shows the results of our long-baseline spectral fitting. Using this technique, we have been able to disentangle two major stellar populations in NGC 5102, and to robustly constrain their ages, metallicities and relative stellar masses, as listed in Table 5. The dominant ($M/M_{gal} = 97\%$) population has an intermediate age (3 Gyr), and super-solar metallicity ($1.5 Z_{\odot}$). Other authors have estimated the age of the younger population, which resides in the nucleus, and these are consistent with the 0.3 Gyr, $0.2 Z_{\odot}$ secondary population that our two-component model fitting finds. The uncertainty contours of the parameters is shown in Figure 6. Results from Pritchett (1979); Rocca-Volmerange & Guiderdoni (1987); Bica (1988) constrain the age to within $\sim 0.1 - 0.5$ Gyr. Bica (1988) also determines that this population has a sub-solar metallicity, $Z = 0.3 Z_{\odot}$.

The age of the older, dominant population in the two-component fit is remarkably young (3 Gyr). In order to check the possibility that there is a sub-population, present within this component, of older (10 Gyr) stars, we have fitted a two-component model to the residual of the spectrum of NGC 5102, following subtraction of the 0.3 Gyr population. Figure 7 shows this residual spectrum, with the best-fitting two-component model overlaid (as in figure 5). The addition of a third, older (10 Gyr, $2.5 Z_{\odot}$) stellar population is not rejected by the fitting statistics, although the increase in the complexity of the model means that the age and metallicity of the third component are not strongly constrained, and we are potentially over-fitting the data. The super-solar abundance found in the oldest component is consistent with other recent estimates of abundances in lenticular galaxies in poor environments (Kuntschner & Davies 1998; Trager, Faber, Worthey, & González 2000; Kuntschner *et al.* 2002) and is therefore not implausible. In order to match the slope of the observed spectrum, the presence of the 10 Gyr population forces the best-fitting younger population to be even younger (2 Gyr). However, even with the addition of the third, oldest component, a substantial

(>~55%) component of the stars must still be young, and relatively high metallicity (Z_{\odot}) in order to fit both the over-all shape of the continuum and the detailed absorption features, especially longwards of 5000 Å, where contributions from more mature (i.e. > 1 Gyr) stars dominate the spectrum, for example, the TiO absorption feature at ~7150 Å. The high metallicity determined for both these two sub-populations indicates the presence of strong absorption features, unambiguously dependent on the metallicity. It should be noted that the feature at ~ 7500 Å is a sky line, which is excluded from the fitting process. Therefore, independent of the model chosen (i.e. either 2-component or 3-component), a large fraction (55-97%) of the stars in NGC 5102 are <3 Gyrs old. If the XRB population is linked directly to the stellar population, this would suggest that NGC 5102 has not had sufficient time to develop an XRB population appropriate to its stellar mass.

We estimate the mass of the youngest (0.3 Gyr) population to be $\sim 2.2 \times 10^7 M_{\odot}$. Again, this is consistent with independent estimates in the literature. Pritchett (1979), using UBVR photometry, estimates that $\sim 2 \times 10^7 M_{\odot}$ stars formed in last ~0.1 Gyr. However, Pritchett's estimate is based on an older estimate of distance, D=4.4 Mpc, from de Vaucouleurs (1975). Using this distance in our more sophisticated mass estimate, we find $\sim 4.4 \times 10^7 M_{\odot}$. An HI survey of NGC 5102 detected a ring of emission with a central depression van Woerden *et al.* (1993). It is interesting that the estimate of the 'missing' mass of this depression is $\sim 1.5 \times 10^7 M_{\odot}$ (D=3.1 Mpc). Although the radial distributions of the HI depression and central starburst differ, the correlation in the masses is suggestive of a link between the HI hole and the formation of the young stellar population. Alternatively, the starburst occurring 0.3 Gyr ago could have been triggered by the capture of a gas-rich dwarf galaxy. There are no sizeable galaxies that are near neighbors with NGC 5102, and it is unlikely that any star-formation-inducing interaction with another large galaxy could have occurred within the last 4 Gyr (van Woerden *et al.* 1993).

5.2. Globular clusters in NGC 5102

We analyzed three archival HST/WFPC2 observations that lie contiguously along the major axis of NGC 5102, obtained with the F569W filter (PI: Freeman). The central pointing consisted of 8 exposures of 500s each, whereas the other two had three exposures of 1100s each. The observations had large overlaps. The effective area we could survey for globular clusters, excluding the central saturated region of the galaxy, was approximately 9.5 sq. arcmin, in a rectangular shape along the major axis. This covered approximately half the optical light of the galaxy covered by the D_{25} ellipse, or ~46% of the total light of the galaxy. We combined the exposures for each field using the DRIZZLE algorithm (Fruchter

& Hook 2002). We then smoothed each combined image I by running a median filter of 16 pixels square, and subtracted a scaled version of the smoothed image S from the original image according to $\alpha I - (\alpha - 1)S$, to produce a unsharp masked image (after trial and error, we chose $\alpha = 16$). Finally, we ran the image finding algorithm SEXTRACTOR to find images that are significantly non-stellar compared to the local PSF, and visually inspected the candidate images.

At the distance of NGC 5102, the mean (King) core radius and tidal radius of a globular cluster (GC) would be approximately 0.15 and 2.8 arcsec. We compared our candidates with those in Holland, Côté, & Hesser (1999), who studied 5 HST/WFPC2 images in the central region of the giant elliptical NGC 5128 (Cen A), at roughly the same distance (3.4 Mpc) as our galaxy. The Holland, Côté, & Hesser (1999) study covered 25 sq. arcmin (6% of the D_{25} ellipse) of NGC 5128, which is 16 times more luminous compared to NGC 5102. In Cen A, they found 21 globular cluster candidates ($r < 2''$) and 61 other extended objects ($r > 2''$), some of which could be single or double GCs. Applying their criterion to our images, we obtained three GC candidates. The positions and ellipticities of these three objects are tabulated in Table 6. Scaling by the fraction of galactic light contained in the HST FOV, we estimate that there are ~ 7 GCs around NGC 5102.

The globular cluster specific frequency (GCSF) is known to be a strong function of both environment and morphological type (see Harris (1991) and references therein). In particular, elliptical galaxies generally have larger GC specific frequencies than lenticular galaxies, and those in richer environments also tend to have larger specific frequencies as well. In addition, the members of the Virgo (e.g. NGC 4472) and Fornax clusters are known to have exceptionally large GCSF values, even for elliptical galaxies in rich environments (van den Bergh 1982). NGC 5102 is a lenticular galaxy, and it resides in a poor environment (it is the fourth most massive galaxy in the Centaurus A group after Cen A, M83, and NGC 4945). The GCSF, S_N , for NGC 5102 is 0.4 if there are 7 GCs, atypically low for lenticular galaxies in poor environments (Harris 1991; Kumai, Hashi, & Fujimoto 1993). A more typical value for the GCSF of ~ 1.5 given the luminosity, morphological type, and environment would imply that there would be ~ 27 GCs. If the number of XRBs scales as the number of GCs (i.e. if all XRBs in early-type galaxies are created in GCs), the deficit of XRBs in NGC 5102 can be accounted for by its low GCSF. For example, there are approximately 1000 GCs around Cen A (Harris *et al.* 2004) and 110 LMXBs within $9'$ with $L_X > 10^{37}$ ergs s^{-1} , or 0.11 XRBs per GC. Thus, we would expect 1 XRB in NGC 5102 given 7 GCs. A similar scaling using XRB and GC populations of NGC 4472 results in the same conclusion.

5.3. High Mass X-ray Binaries

Given the recent star formation in NGC 5102, it is possible that some or all of the XPSs are actually HMXBs; either wind accretors with main sequence secondaries like Cen X-3 or Cyg X-1, or Be star binaries like X Per. The relatively low luminosity ($\sim 10^{36}$ ergs s^{-1}) of the majority of XRBs in NGC 5102 is more consistent with the population of HMXBs in our galaxy, than of the LMXBs (Grimm, Gilfanov, & Sunyaev 2002). For galaxies with a large on-going star formation rate, it has been argued that a significant fraction of the XPS population are HMXBs (Grimm, Gilfanov, & Sunyaev 2003). The lifetime of objects such as Cyg X-1 and Cen X-3 is short (a few $\times 10^7$ yrs), but not less than the estimated time since the last burst of star formation in NGC 5102 ($\sim 1.5 \times 10^7$ yrs (Deharveng *et al.* 1997)). Such objects are rare in our galaxy in large part because of their short lifetimes and the fact that they require the original masses of both progenitor stars to be fairly large (Verbunt 1996, 2001).

It is more likely that if any of the objects in NGC 5102 are HMXBs, they are Be star X-ray binaries. Given the transient nature of such sources, it is possible that there is a large population of such objects in NGC 5102 that are currently not detectable. Deharveng *et al.* (1997) resolved a population of ~ 30 blue stars, mostly likely B main sequence stars, but possibly post-AGB stars, in the central $7''$ of the galaxy with the HST Faint Object Camera. The distribution of the stars in this region follows the light distribution, so that even beyond this central region, it is possible that the sources are HMXBs. A correlation between the XPSs and the HII regions would support this, but as stated above, there are no such coincidences. A detailed optical follow-up of the X-ray sources would resolve this issue. We emphasize that if some or all of the XPSs in NGC 5102 turn out to be HMXBs, this makes the LMXB discrepancy between NGC 5102 and more massive ellipticals even larger as it is unlikely that a significant fraction of the XPSs in this latter group are HMXBs.

High mass X-ray binaries with an OB supergiant companion have been observed in our galaxy to have large (60-100 km s^{-1}) velocities (Chevalier & Ilovaisky 1997). Such an object will only be marginally bound to this relatively low mass galaxy, and would travel ~ 1 kpc in 10^7 yrs. It is therefore possible that one (or more) of the XPSs in the halo NGC 5102 are such objects. Be stars are generally created with smaller velocities, but may be somewhat longer lived. These halo sources could be Be star binaries as well. We noted above that there is a group of seven sources several kpc to the north of the nucleus with no obvious counterparts in the J-band 2MASS image (see Figure 2). One or more of these may be such a halo HMXB ejected from the galaxy. Again, a detailed optical follow-up of the sources would confirm or refute this.

6. Discussion

We have demonstrated that the previously known low X-ray luminosity of NGC 5102 is the result of a deficit of XRBs coupled with a modest amount of hot gas. We have also shown that more than half of the stars in this unusually blue lenticular galaxy are less than 2-3 Gyrs old, and that NGC 5102 has an unusually small number of globular clusters. Is the lack of XRBs related to the relative youth of the stellar population, to the lack of GCs, or both? It is impossible to draw any definitive conclusion based on a sample of one galaxy and the small number of X-ray sources detected. There is little doubt that GCs play an important role in the formation of XRBs in early-type galaxies. The question, though, is what role does the stellar population play. It is probable that both the star formation history and the deficit of GCs play a role in the lack of XRBs in NGC 5102.

Even if 30-60% of the XRBs in all early-type galaxies are contained within GCs, the other 40-70% of the population remains unaccounted for. It is possible that all XRBs in early-type galaxies were formed in GCs and have been ejected, although there is little evidence to either support or refute this claim. On the other hand, this non-GC XRB population may represent an entirely distinct group of sources. Given the LMXB population in the Milky Way and M31 bulges, it would be surprising if most of these sources were not formed via the stellar evolution scenario described above. A study of the XRB populations of a sample of early-type galaxies with different star formation histories is required to address this question. If the XRB population is directly linked to the star formation history, our results would suggest that the stellar population must evolve sufficiently for a significant XRB population to form, and that there is a minimum timescale of a few Gyrs for XRB activity to commence. This timescale is roughly consistent with estimates of the timescale required for rotational braking of the magnetic winds of companion stars to extract orbital angular momentum and therefore reduce the orbital separation of a post-supernova binary to the point where Roche lobe overflow occurs and an LMXB is formed (Verbunt & Zwaan 1981).

One important, more general consequence of a relationship between the LMXBs and the star formation history would be that the X-ray luminosity of a galaxy should peak several gigayears after any massive burst of star formation (White & Ghosh 1998). Most of the star formation in galaxies is believed to have taken place at $z \sim 1-2$ or earlier (Blaine *et al.* 1999). White & Ghosh (1998) calculate that the X-ray luminosity of galaxies should peak at $z \sim 0.5-1$. Chandra observations of the Hubble Deep Field North of the X-ray flux from optically bright spiral galaxies support this hypothesis (Brandt *et al.* 2001; Ptak *et al.* 2001), which can be generally extended to galaxies of all morphological types (Ghosh & White 2001). This temporal evolution of the XRB population would be hard to explain if it were entirely

linked to the GC population. Clearly there is an important relationship between the LMXBs and the GC population for the most massive elliptical galaxies in rich environments with large GCSFs. However, the SFR history and binary evolution must also play an important role in the formation of LMXBs. We are currently investigating the relationship between the XRB population, the star formation history (via the spectral synthesis technique), and the globular cluster population in a large sample of early-type galaxies, the results of which will be presented in a future publication.

This work was funded by NASA grant GO2-3109X.

REFERENCES

- Angelini, L., Loewenstein, M., & Mushotzky, R. F. 2001, ApJ, 557, L35.
- Athey, A. 2003, Ph. D. thesis, University of Michigan.
- Bica, E. 1988, A&A, **195**, 76.
- Bica, E. & Alloin, D., 1987a, A&A, **70**, 28.
- Bica, E. & Alloin, D., 1987b, A&A, **186**, 49.
- Blain, A. W., Jameson, A., Smail, I., Longair, M. S., Kneib, J.-P., & Ivison, R. J. 1999, MNRAS, **309**, 715.
- Brandt, W. N., *et al.* 2001, AJ, **122**, 1.
- Calzetti, D., Kinney, A.L. & Storchi-Bergmann 1994, ApJ, **429**, 582.
- Calzetti, D. 1997, AJ, **113**, 162.
- Canizares, C. R., Fabbiano, G., & Trinchieri, G 1987, ApJ, **312**, 503.
- Chevalier, C. & Ilovaisky, S. A. 1997, A&A, **330**, 201.
- David, L. P., Forman, W. R., & Jones, C. 1990, ApJ, **359**, 29.
- David, L. P., Forman, W. R., & Jones, C. 1990, ApJ, **369**, 121.
- Deharveng, J.-M., Jedrzejewski, R., Crane, P., Disney, M. J., & Rocca-Volmerange B., A&A, **326**, 528.
- de Vaucouleurs, G., 1975, in *Galaxies and the Universe*, ed. A. Sandage and J. Christian (Chicago: University of Chicago Press), p. 557.
- de Vaucouleurs *et al.* 1991, “Third Reference Catalog of Bright Galaxies”, Springer-Verlag (New York).
- Fabbiano, G., Krauss, M., Zezas, A., Rots, A., Neff, S. 2003, ApJ, **598**, 272.
- Forman, W. R., Jones, C., & Tucker, W. 1985, ApJ, **293**, 102.
- Fruchter, A. S. & Hook, R. N. 2002, PASP, 114, 144.
- Ghosh, P. & White, N. 2001, ApJ, 559, L97.

- Grimm, H.-J., Gilfanov, M., & Sunyaev, R. 2002, *A. & A.*, **391**, 923.
- Grimm, H.-J., Gilfanov, M., & Sunyaev, R. 2003, *MNRAS*, **339**, 793.
- Grimm, H.-J., Zezas, A., & Fabbiano, G. 2004, *HEAD/AAS*, 25.06.
- Harris, W. E. 1991, *ARA&A*, **29**, 543.
- Harris, G. L. H. *et al.* 2004, *AJ*, **128**, 712.
- Holland, S., Côté, P., & Hesser, J. E. 1999, *A&A*, 348, 418.
- Irwin, J. A. & Bregman, J. N. 2004, *BAAS*, 203.5201.
- Irwin, J. A. & Sarazin, C. L. 1998, *ApJ*, **499**, 650.
- Israel, F. P. 1998, *Astron. Astrophys. Rev.*, **8**, 237.
- Jimenez R., Padoan P., Matteucci F., & Heavens A.F. 1998, *MNRAS*, **229**, 123.
- Kalogera, V. & Webbink, R. F. 1996, *ApJ*, **458**, 301.
- Kalogera, V. & Webbink, R. F. 1998, *ApJ*, **493**, 351.
- Kenter, A. T., & Murray, S. M. 2003, *ApJ*, **584**, 1016.
- Kim, D.-W., Fabbiano, G., & Trinchieri, G. 1992, *ApJ*, **393**, 134.
- Kong, A. K. H., DiStefano, R., Garcia, M., & Greiner, J. 2003, *ApJ*, **585**, 298.
- Kraft, R. P., Kregenow, J. M, Jones, C., Forman, W. R., & Murray, S. S. 2001, *ApJ*, **560**, 675.
- Kraft, R. P., *et al.* 2005, in preparation.
- Kumai, Y., Hashi, Y., & Fujimoto, M. 1993, *ApJ*, **416**, 576.
- Kundu, A., Maccarone, T. J., & Zepf, S. E. 2002, *ApJ*, **574**, L5.
- Kuntschner, H. & Davies, R. L. 1998, *MNRAS*, **295**, L29.
- Kuntschner, H., Smith, R. J., Colless, M., Davies, R. L., Kaldare, R., & Vazdekis, A. 2002, *MNRAS*, **337**, 172.
- Maccarone, T. J., Kundu, A., & Zepf, S. E. 2003, *ApJ*, 586, 814.

- Matsumoto, H., Koyama, K., Awaki, H., Tsuru, T., Loewenstein, M., & Matsushita, K. 1997, *ApJ*, **482**, 133.
- McMillan, R., Ciardullo, R., & Jacoby, G. H. 1995, *AJ*, **108**, 1610.
- Minniti, D., Rejkuba, M., Funes, J. G. S. J., & Akiyama, S. 2004, *ApJ*, **716**, 600.
- O’Sullivan, E., Forbes, D. A., & Ponman, T. J. 2001, *MNRAS*, **328**, 461.
- Pritchett, C. 1979, *ApJ*, **231**, 354.
- Ptak, A., *et al.* 2001, *ApJ*, **559**, L91.
- Rocca-Volmerange, M., & Guiderdoni, B. 1987, *A&A*, **175**, 15.
- Sarazin, C., Irwin, J. A., & Bregman, J. N. 2000, *ApJ*, **544**, L101.
- Tozzi, P. *et al.* 2001, *ApJ*, **562**, 42.
- Trager, S. C., Faber, S. M., Worthey, G., & González, J. J. 2000, *AJ*, **119**, 1645.
- van den Bergh, S. 1976, *AJ*, **81**, 795.
- van den Bergh, S. 1982, *PASP*, **94**, 459.
- van Woerden, H., van Driel, W., Braun, R., & Rots, A.H. 1993, *A&A*, **269**, 15.
- Verbunt, F. & Zwaan, C. 1981, *A&A*, **100**, L7.
- Verbunt, F. 1996, ‘The Formation of Neutron Star and Black Hole Binaries’, *Proc. NATO Advanced Study Institute*, ed. by R. A. M. J. Wijers and M. B. Davies, Dordrecht, Kluwer Academic Publishers.
- Verbunt, F. 2001, ‘Formation and Evolution of Black Hole Binaries’, *Proc. ESO Workshop*, ed. by L. Kaper, E. P. J. van den Heuvel, and P. A. Woudt, Springer.
- Webbink, R. F., Rappaport, S., & Savonijie, G. J. 1983, *ApJ*, **270**, 678.
- White, N., & Ghosh, P. 1998, *ApJ*, **504**, L31.
- White, R. E., Sarazin, C. L., & Kulkarni, S. R. 2002, *ApJ*, 571, L23.
- Wu, K. 2001, *Publ. Astron. Soc. Austr.*, **18**, 443.

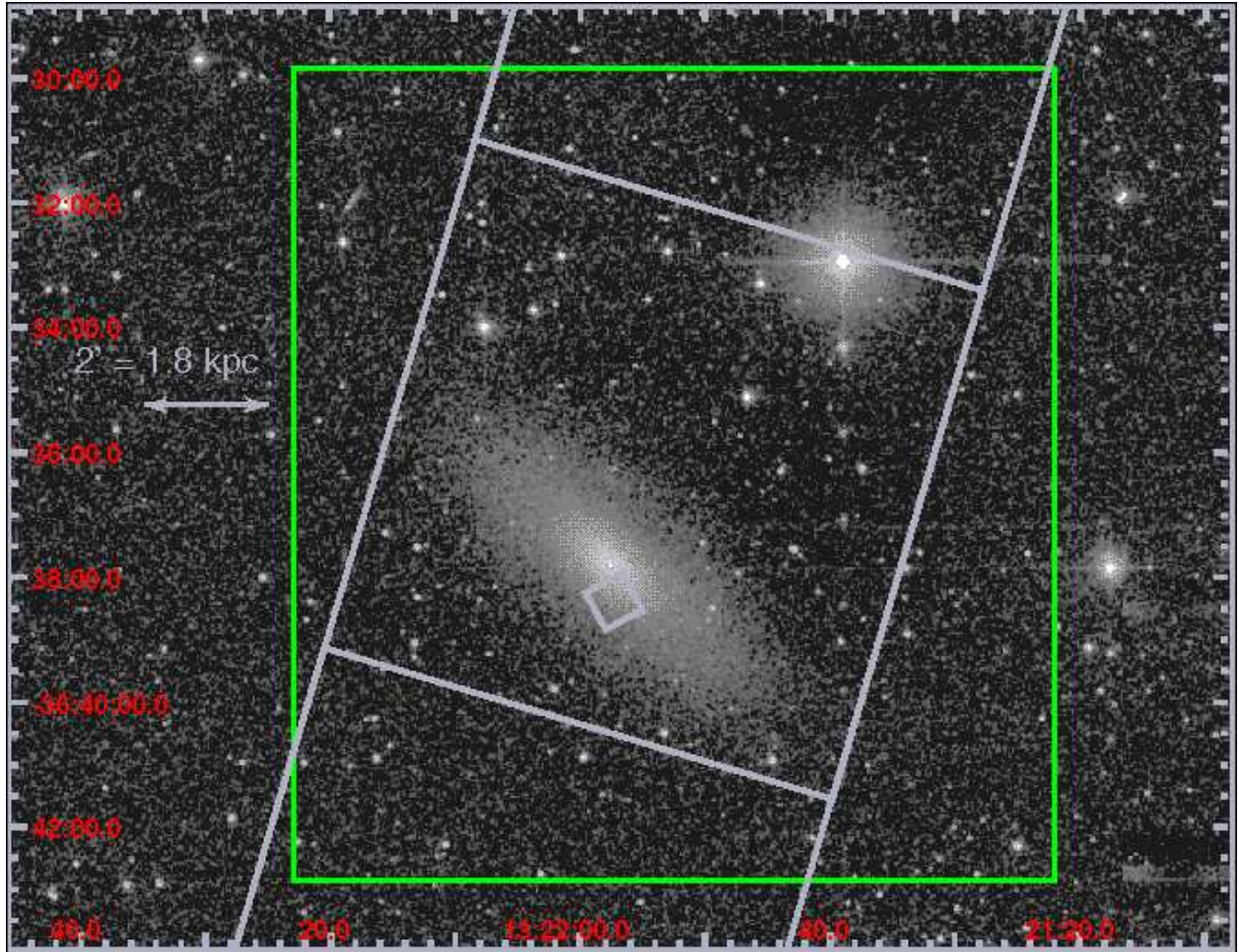


Fig. 1.— The Chandra/ACIS-S FOV overlaid onto a 2MASS J band image of NGC 5102. North is up, east is to the left. The coordinates in this and all other figures are J2000. The diamond in the center of the image is the position of best focus on the S3 chip, The chips to the NNE and SSW are the S4 and S2 chips, respectively. The green box denotes the boundary of the region searched for point sources.

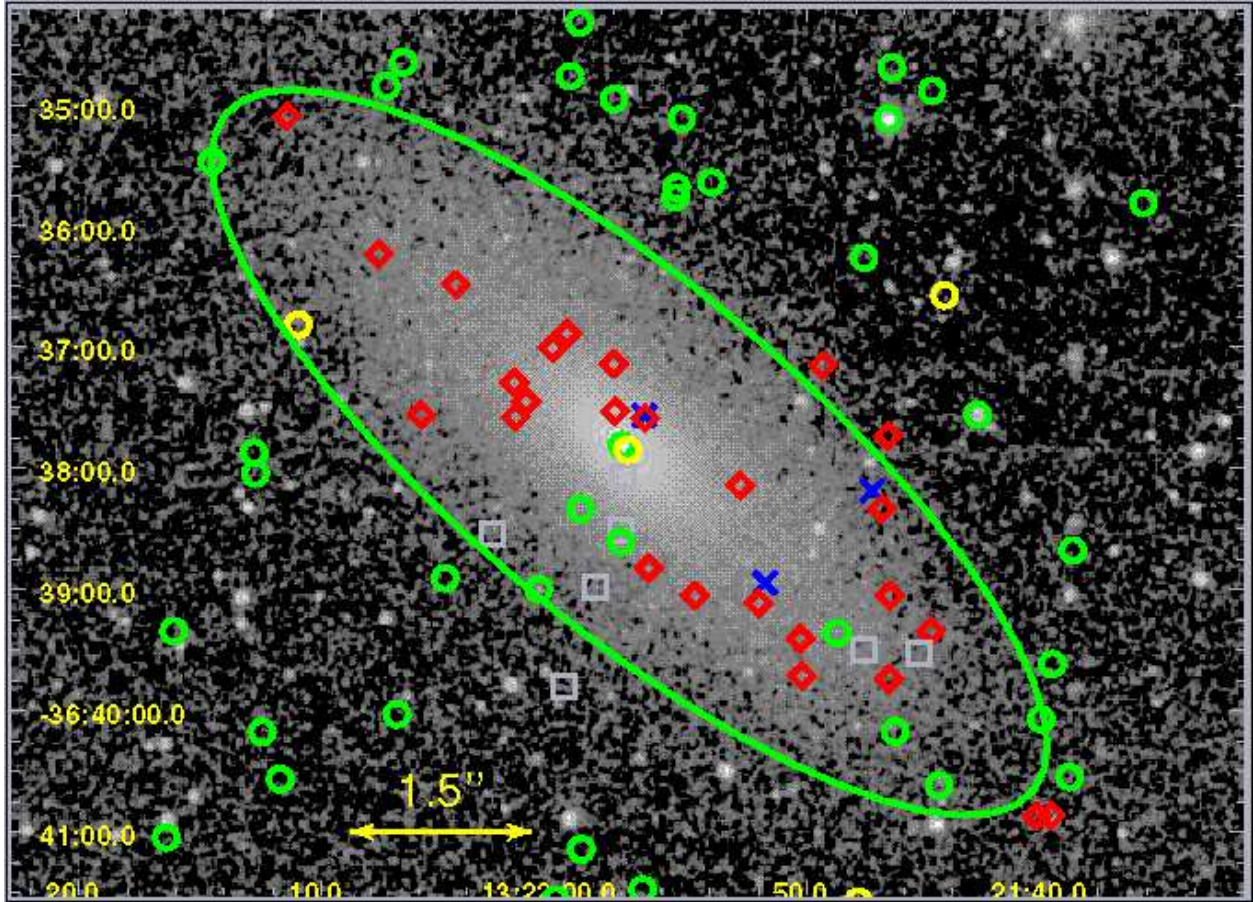


Fig. 2.— Positions of the X-ray points sources overlaid onto a 2MASS J band image of NGC 5102. The large green ellipse denotes the optical boundary (D_{25}) of the galaxy, the yellow and green circles the XPSs with $L_X \geq 10^{37}$ ergs s^{-1} and $L_X < 10^{37}$ ergs s^{-1} , respectively, the red diamonds are planetary nebulae, and the white boxes are HII regions (the later two taken from McMillan, Ciardullo, & Jacoby (1995)). The blue Xs represent GC candidates.

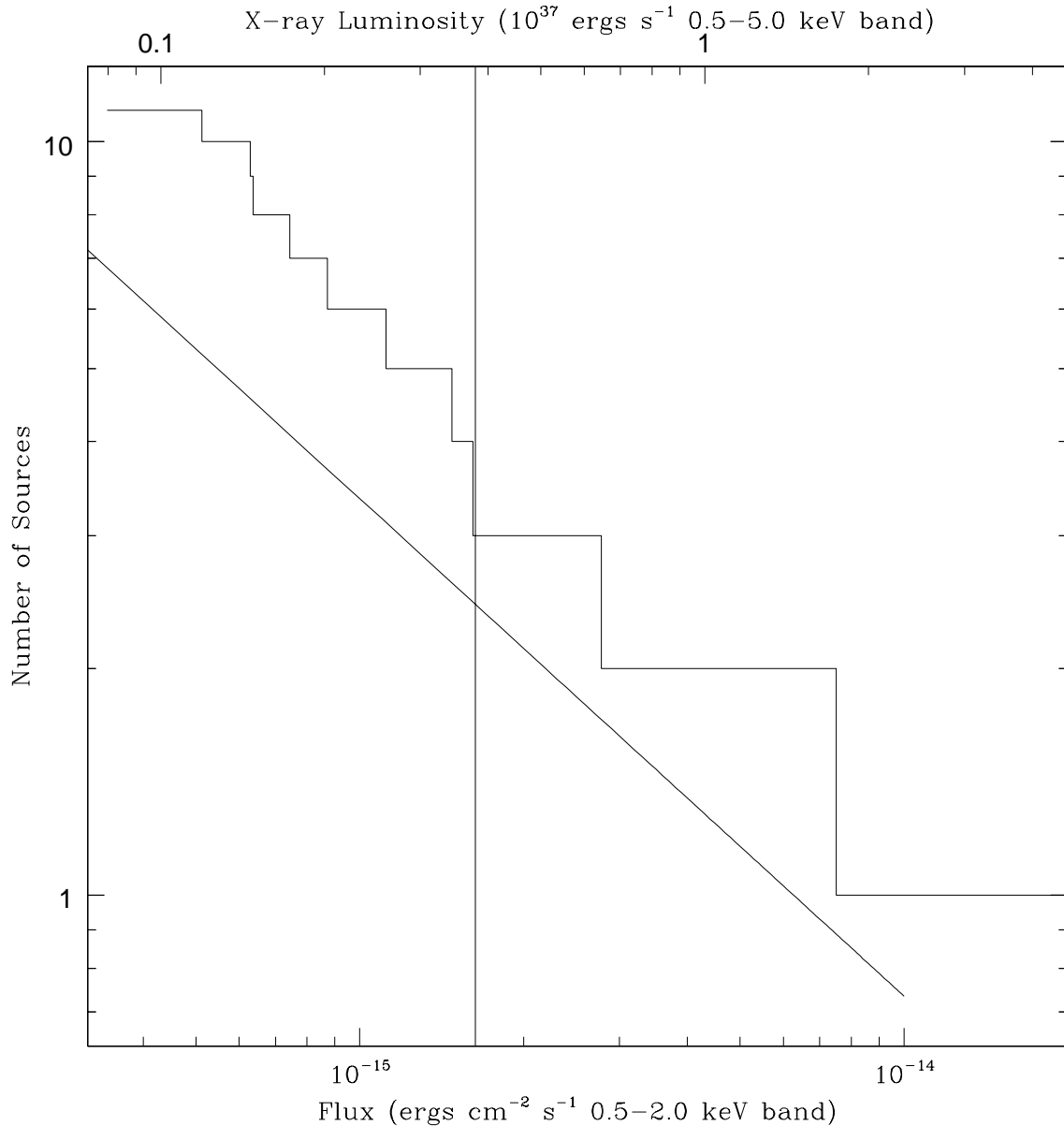


Fig. 3.— Cumulative luminosity function (the histogram) of X-ray point sources detected in elliptical region (within the D_{25} isophote) described in text. The $\log(N)$ - $\log(S)$ of the background AGN is plotted as the continuous curve (Tozzi *et al.* 2001). The corresponding X-ray luminosity of the sources in the 0.5–5.0 keV band (assuming the source to be at a distance of 3.1 Mpc) is shown across the top. The solid vertical line denotes the flux corresponding to 16 counts in our observation. Above this line, we are complete and unbiased (see text for detailed discussion).

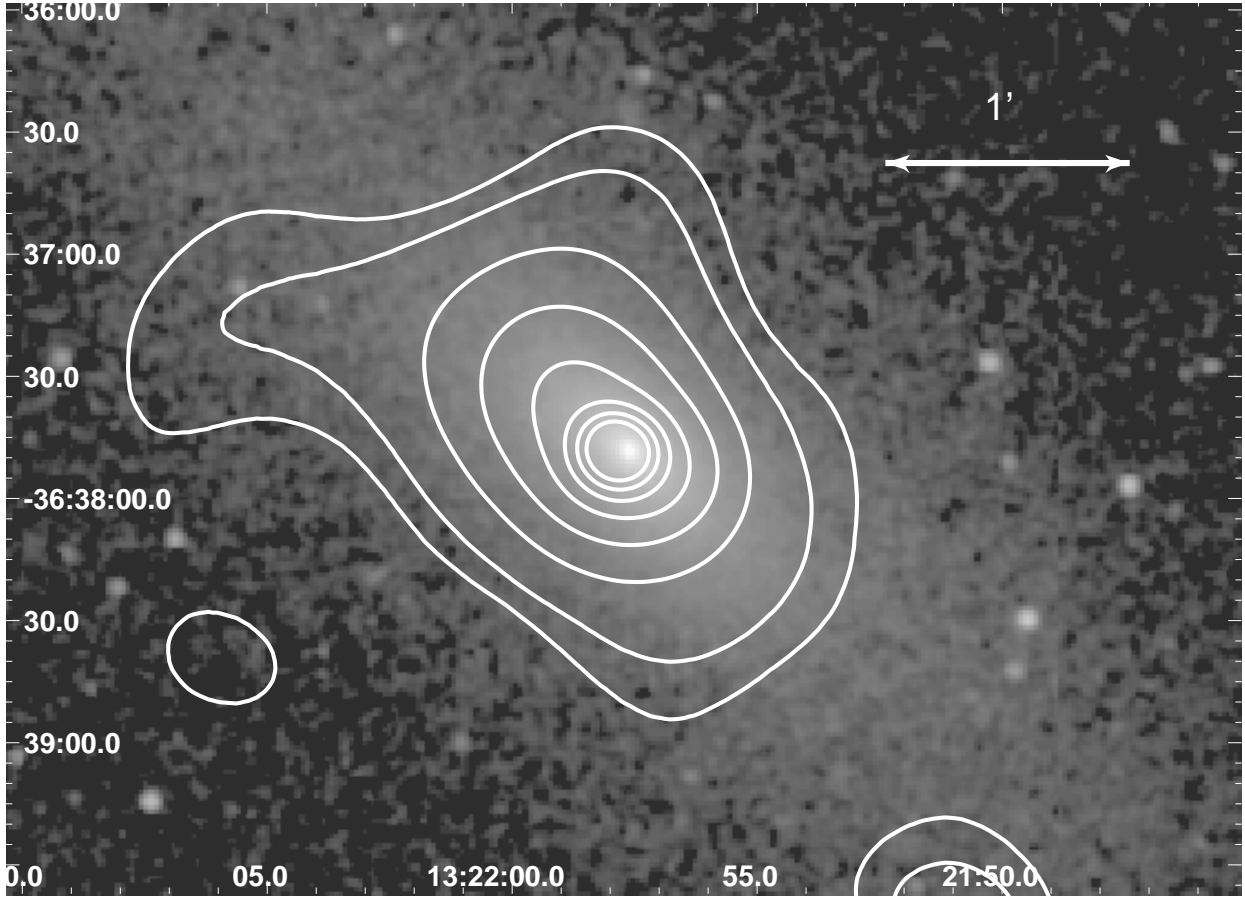


Fig. 4.— Contours from adaptively smoothed, exposure corrected, background subtracted X-ray image of NGC 5102 in the 0.5-2.0 keV band overlaid onto a 2MASS J band image. The contours correspond to X-ray count rates of 1.0, 1.5, 2.8, 4.9, 7.9, 11.7, 16.4, and 22.0×10^{-7} cts arcsec $^{-2}$ s $^{-1}$ above background.

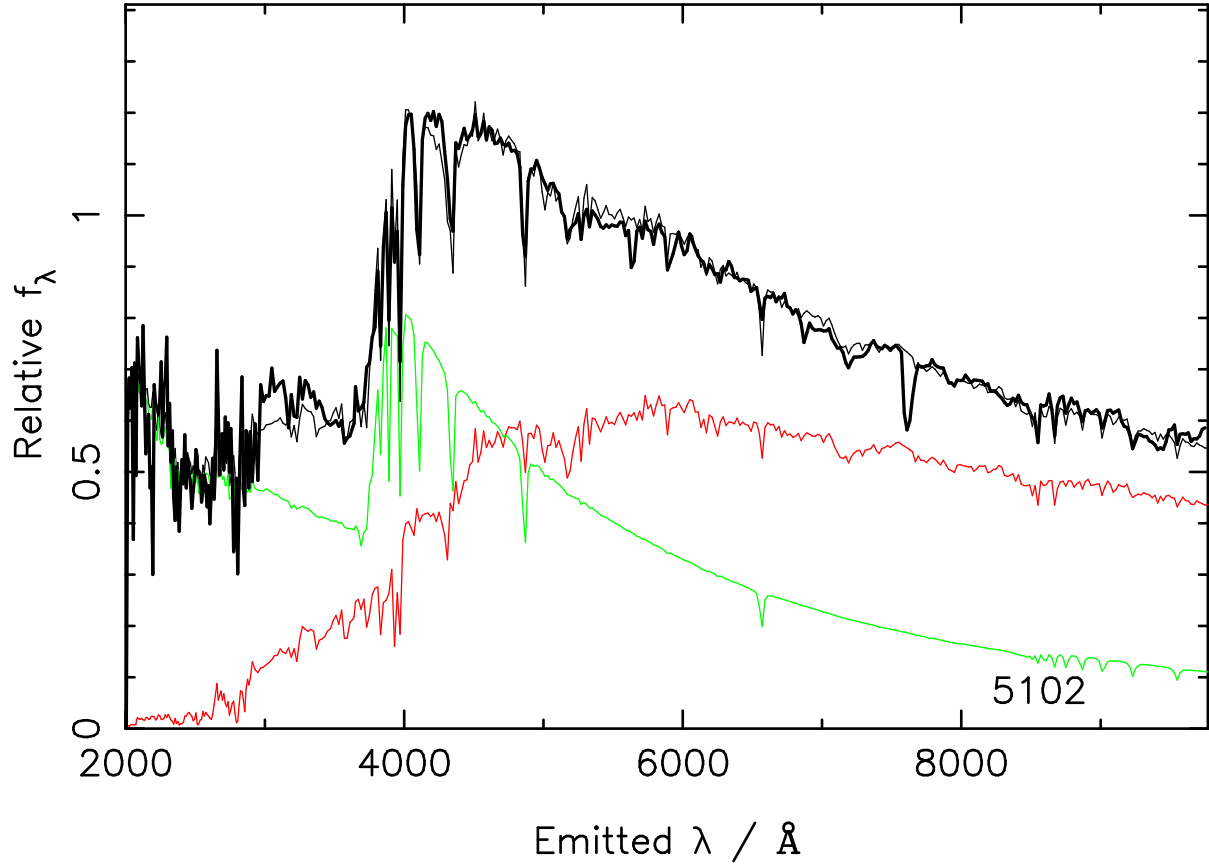


Fig. 5.— The best-fitting two-component model (thin black line) superimposed over the spectrum of NGC 5102 (thick black line). The two component populations are also shown; the dominant population (3 Gyr, $Z = 1.5 Z_\odot$) is in red, and the lesser population (0.3 Gyr, $Z = 0.2 Z_\odot$) is in green.

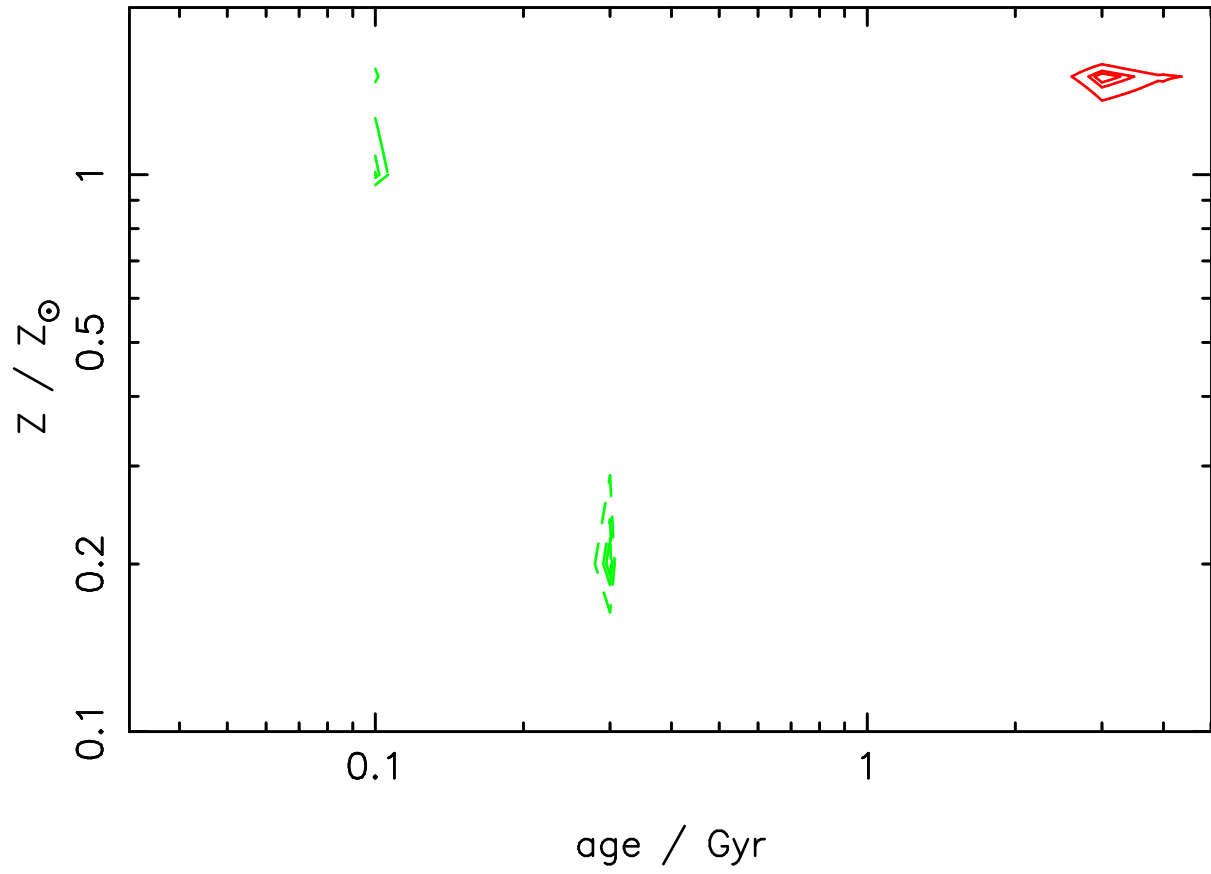


Fig. 6.— Contour plot of constant relative likelihood. The contours contain 68.3%, 90% and 95.4% relative likelihood. The dominant population contours are in red, and the secondary population contours are green.

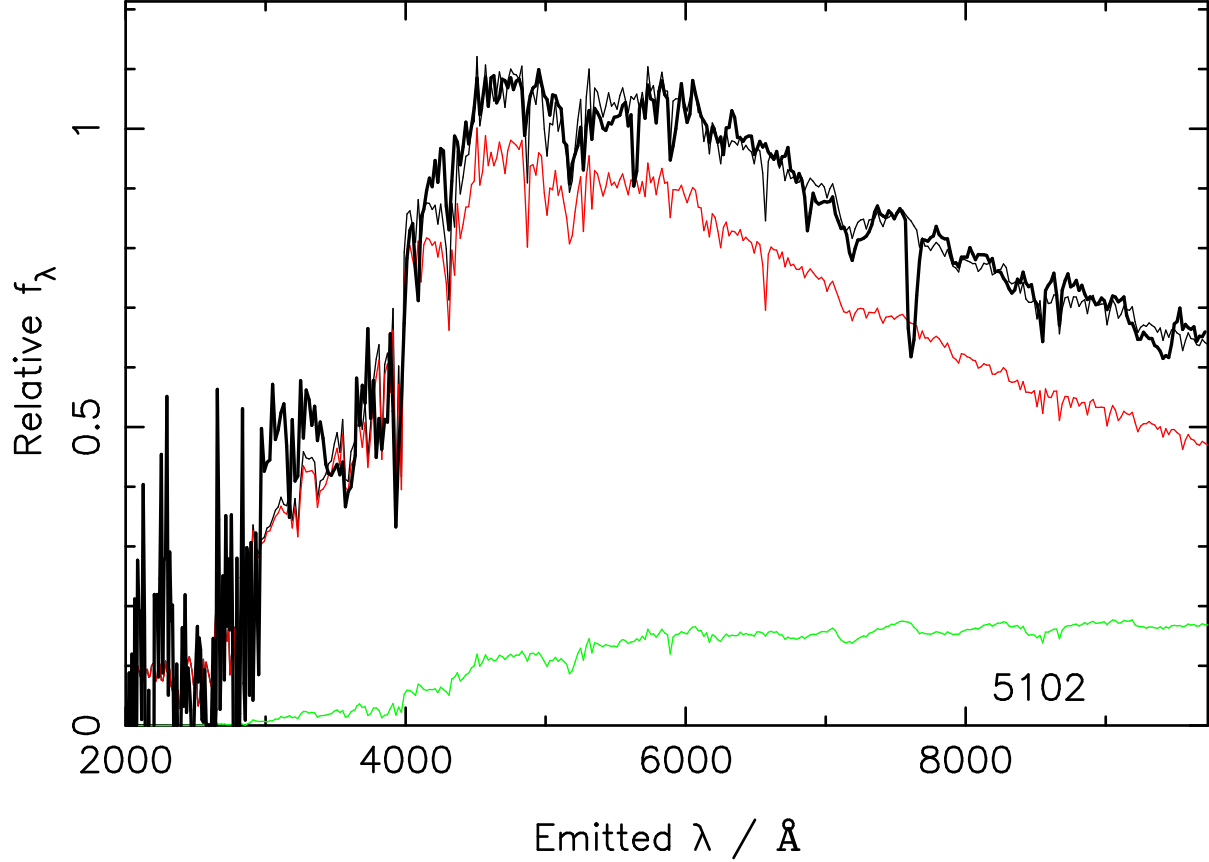


Fig. 7.— The best-fitting two-component model (thin black line) superimposed over the residual of the spectrum of NGC 5102, following subtraction of the 0.3 Gyr population (thick black line). The two component populations are also shown; the dominant population is in red (2 Gyr, $Z = Z_{\odot}$), and the lesser population (10 Gyr, $Z = 2.5 Z_{\odot}$) is in green. A faint population of older (10 Gyr) stars is not rejected by the fitting statistics.

Parameter	Value
Position (J2000)	
RA	$13^h 21^m 57.6^s$
Dec	$-36^d 37^m 49^s$
Optical Properties	
m_B	9.99
$B - V$	0.64
Distance	3.1 ± 0.15 Mpc
L_B	$1.49 \times 10^9 L_\odot$
Chandra Observation Log	
Date	21MAY02
Exposure Time	34217 s
OBSID	2949

Table 1: Summary of parameters for NGC 5102.

Source	RA	DEC	Rate (10^{-4} cts s^{-1})	$\log(L_X)$
1	13:21:36.16	-36:35:48.8	2.9 ± 1.0	
2	13:21:38.97	-36:34:05.9	5.8 ± 1.5	
3	13:21:39.07	-36:38:40.7	4.5 ± 1.2	
4	13:21:39.19	-36:40:32.9	9.3 ± 2.3	
5	13:21:39.91	-36:39:37.0	4.9 ± 1.3	
6	13:21:40.36	-36:40:04.3	2.2 ± 0.9	36.24
7	13:21:42.99	-36:37:33.5	2.0 ± 0.8	
8	13:21:44.35	-36:36:34.5	14.9 ± 2.2	
9	13:21:44.56	-36:40:37.1	4.2 ± 1.2	36.53
10	13:21:44.86	-36:34:53.1	1.6 ± 0.7	
11	13:21:46.29	-36:33:54.1	14.9 ± 2.2	
12	13:21:46.38	-36:40:10.5	1.7 ± 0.7	36.15
13	13:21:46.52	-36:34:41.7	2.4 ± 0.9	
14	13:21:46.67	-36:35:07.1	5.5 ± 1.3	
15	13:21:47.66	-36:36:15.9	1.2 ± 0.6	
16 [†]	13:21:47.88	-36:41:34.6	10.2 ± 2.0	
17	13:21:48.76	-36:39:21.7	2.3 ± 0.9	36.28
18 [†]	13:21:51.86	-36:30:50.8	2.3 ± 1.1	
19	13:21:52.12	-36:33:09.1	7.9 ± 1.7	
20	13:21:53.04	-36:32:47.9	7.0 ± 1.6	
21	13:21:53.94	-36:35:38.5	3.1 ± 1.0	
22 [†]	13:21:54.98	-36:41:42.9	6.1 ± 1.5	
23	13:21:55.16	-36:35:06.9	9.0 ± 1.6	
24	13:21:55.37	-36:35:41.1	3.7 ± 1.1	
25	13:21:55.43	-36:35:46.0	6.3 ± 1.4	
26 [†]	13:21:56.78	-36:41:28.8	6.8 ± 1.6	
27	13:21:57.40	-36:37:51.0	33.8 ± 3.2	37.44
28	13:21:57.63	-36:37:48.8	4.4 ± 1.2	36.55
29	13:21:57.67	-36:38:36.5	1.1 ± 0.6	35.97
30	13:21:57.96	-36:34:57.3	3.9 ± 1.1	
31 [†]	13:21:59.30	-36:41:08.8	1.9 ± 0.9	
32	13:21:59.33	-36:38:20.3	1.7 ± 0.7	36.13
33	13:21:59.37	-36:34:19.5	2.1 ± 0.8	
34	13:21:59.76	-36:34:46.0	5.6 ± 1.3	
35 [†]	13:22:00.35	-36:41:33.7	3.4 ± 1.2	
36	13:22:01.05	-36:39:00.1	1.7 ± 0.7	36.15
37 [†]	13:22:01.59	-36:30:38.4	9.0 ± 2.4	
38 [†]	13:22:04.45	-36:42:20.0	1.5 ± 0.8	
39	13:22:04.91	-36:38:54.6	5.2 ± 1.2	
40 [†]	13:22:06.05	-36:30:49.1	108.4 ± 11.0	
41	13:22:06.62	-36:34:39.1	1.4 ± 0.7	
42 [†]	13:22:06.89	-36:40:02.0	3.6 ± 1.2	

43	13:22:07.32	-36:34:50.9	5.9 ± 1.4	
44	13:22:07.32	-36:33:23.7	2.3 ± 0.9	
45	13:22:07.68	-36:34:00.1	1.9 ± 0.8	
46	13:22:10.94	-36:36:49.0	12.4 ± 2.0	37.00
47†	13:22:11.71	-36:40:34.0	1.9 ± 0.9	
48†	13:22:12.45	-36:40:10.7	1.1 ± 0.7	
49	13:22:12.71	-36:38:02.8	7.5 ± 1.5	
50	13:22:12.76	-36:37:52.5	11.6 ± 1.9	
51	13:22:14.50	-36:35:28.1	3.6 ± 1.3	36.46
52†	13:22:14.97	-36:42:43.5	8.2 ± 2.0	
53†	13:22:15.49	-36:41:57.2	27.7 ± 3.5	
54	13:22:16.09	-36:39:20.6	1.9 ± 1.1	
55†	13:22:16.40	-36:41:03.0	3.2 ± 1.2	

Table 2:: Summary of X-ray point sources around NGC 5102. The count rates and uncertainties are in the 0.5-5.0 keV band. The X-ray luminosities are given for those sources that are within the optical D_{25} isophote (see text for complete discussion) assuming a distance of 3.1 Mpc. The sources labeled with a dagger lie on the S2 or S4 chips, none of which are within the D_{25} isophote.

Galaxy	m_B	m_J	Distance (Mpc)	M_B	M_J	N_{XPS}
NGC 4472	9.33	6.27	16.0	-21.69	-24.75	~ 220
NGC 5128	7.30	4.98	3.5	-20.24	-22.76	~ 110
NGC 5102	9.97	7.71	3.1	-17.49	-19.75	5(est.)/1(obs.)

Table 3: Comparison of optical/IR properties of NGC 5102, NGC 5128 (Cen A), and NGC 4472.

source	wavelength range - Å
IUE Newly Extracted Spectra	2000-3200
Bica & Alloin, unpublished	3100-5400
Bica & Alloin (1987a)	3800-7500
Bica & Alloin (1987b)	6400-9800

Table 4: Sources of the archival spectra of NGC 5102. The Bica & Alloin data are available at <ftp://cdsarc.u-strasbg.fr/cats/III/219/>.

age / Gyr	Z / Z _⊙	M / M _{gal}	minimum χ^2_ν	k
3.0	1.5	0.93	174.7/430	0.10
0.3	0.2	0.07		

Table 5: The results of fitting the near-UV-to-optical spectra of NGC 5102 with the two-component model spectrum. The parameters quoted are those values on the age-metallicity grid which correspond to the minimum calculated χ^2 . The age and metallicity of the two-component populations are given, for the best fitting combination for each model set. M / M_{gal}, the fractional contribution, by mass, to the total population made by each component is shown in column 3, and the dust extinction parameter, k , is given in column 5.

Globular cluster candidates		
13:21:51.73	-36:38:56.9	0.066
13:21:47.33	-36:38:11.2	0.149
13:21:56.71	-36:37:34.1	0.261

Table 6: Positions (J2000) and ellipticities ($1 - b/a$) of globular cluster candidates detected in HST observations.